BIOCELL
2023 47(6): 1293-1306

Tech Science Press

Bioinformatic analysis of lncRNA-associated competing endogenous RNA regulatory networks in synovial tissue of temporomandibular joint osteoarthritis

Chuyao WANG[1,2,#]; Chuan LU[2,#]; Luxiang ZOU[2,*]; Dongmei HE[2,*]

[1] School of Stomatology, Qingdao University, Qingdao, 266000, China
[2] Department of Oral Surgery, Ninth People's Hospital, Shanghai Jiao Tong University School of Medicine, Shanghai Key Laboratory of Stomatology & Shanghai Research Institute of Stomatology, National Clinical Research Center of Stomatology, Shanghai, 200011, China

Key words: TMJOA, Non-coding RNAs, Osteoarthritis prevention and treatment

Abstract: Background: Temporomandibular joint osteoarthritis (TMJOA) is an end-stage disease that seriously affects the patients' quality of life. Molecular insights in advancing our understanding of TMJOA are the need of the hour. **Methods:** We performed RNA high-throughput sequencing and bioinformatics analysis of differentially expressed (DE) long non-coding RNA (lncRNAs), microRNAs (miRNAs), and messenger RNA (mRNAs) in human synovial TMJOA tissues. Firstly, synovium samples of TMJOA patients and non-TMJOA controls were collected for high-throughput sequencing of lncRNAs, miRNAs, and mRNAs. We then performed biological function analysis of the top 100 mRNAs with more than 2-fold differential expression, and their upstream regulated miRNAs and lncRNAs were predicted separately. Intersections between predicted miRNAs/lncRNAs and differentially expressed miRNAs/lncRNAs were determined, respectively. Regulatory networks among the selected lncRNAs, miRNAs, and mRNAs were constructed. Finally, Western Blotting and reverse transcription-quantitative polymerase chain reaction (RT-qPCR) were used to explore the function of selected lncRNA and mRNAs. **Results:** Our analysis showed that the only upregulated lncRNA*xist*, was involved in intracellular protein degradation, cartilage matrix degradation, and osteoclast differentiation through four regulatory axes: *miR-1271-5p/ctsb*, *miR-365a-3p/mmp3*, *miR-199a-3p/fos*, and *miR-27b-3p/miR-1271-5p/grb2*. RT-qPCR results showed that *xist* expression increased in both TMJOA synovial tissue and inflammatory-stimulated synovial cells. Inhibition of *xist* could promote the proliferation of synovial cells upon inflammatory stimulation, and *xist* could positively regulate the expression of GRB2. Targeting GRB2 could inhibit the expression of matrix degrading enzymes in synovial cells, thereby attenuating the inflammatory environment. **Conclusion:** Given the current lack of reports of lncRNA regulation in TMJOA synovitis, our results revealed that *xist* was significantly differentially expressed in human synovial TMJOA and could regulate the expression of GRB2, which may play a role in the progression of TMJOA.

Introduction

Temporomandibular joint osteoarthritis (TMJOA) is an end-stage disease of temporomandibular joint disorder (TMD) characterized pathologically by synovial inflammation, cartilage degeneration, and subchondral bone remodeling. The clinical manifestations include chronic pain and masticatory difficulties that seriously affect a patient's quality of life (Bush and Beier, 2013; Li *et al.*, 2019). Although there are many studies on the etiology of TMJOA, its exact pathogenesis remains unclear (Zheng *et al.*, 2018).

In recent years, studies on RNA sequencing have found that a variety of noncoding RNAs, including miRNA, lncRNA, and circRNA play an important role through competing endogenous RNA (ceRNA) networks in the development of osteoarthritis (OA) (Kostopoulou *et al.*, 2015; Yin *et al.*, 2017). CircRNAs and lncRNAs can act as endogenous miRNA molecular sponges and competitively inhibit miRNA regulation of target mRNAs (Memczak *et al.*, 2013; Wang *et al.*, 2016; Zheng *et al.*, 2016; Wang *et al.*, 2017; Xiong *et al.*, 2018). Our previous study found that the

*Address correspondence to: Dongmei He, lucyhe119@163.com
#Co-first authors
Received: 04 December 2022; Accepted: 15 February 2023;
Published: 22 May 2023

Doi: 10.32604/biocell.2023.028199

expression of circRNA*gcn1l1* was elevated in synovial TMJOA tissues and was able to regulate Tumor Necrosis Factor-alpha (TNF-a) secretion by synoviocytes through *miRNA-330-3p*, aggravating cartilage degeneration (Zhu *et al.*, 2020). LncRNAs are another important group of miRNA sponges in addition to circRNAs and may be an important therapeutic target of TMJOA as an indispensable part of ceRNA regulation. For example, Fu *et al.* (2021) found that the lncRNA-*h19/miR-124a/cdk2/mcp-1* axis could promote the proliferation of human rheumatoid arthritis (RA) synoviocytes and synovial inflammation, which may represent a new RA therapeutic strategy. Bi *et al.* (2019) concluded that inhibition of lncRNA *picsar/miRNA-4701-5p* could effectively inhibit the proliferation and invasion of synoviocytes as well as secretion of inflammatory factors in human RA. Thus, lncRNA *picsar* could be used as a new biomarker for RA. In addition, the lncRNA *neat1/miRNA-204-5p/NF-κB* axis and the lncRNA *pint/miRNA-155-5p/socs1* axis have also been reported in human RA synovitis symptoms (Wang and Zhao, 2020; Xiao *et al.*, 2021).

As there is a current lack of reports on lncRNA regulation in TMJOA synovitis, in this study, we performed high-throughput sequencing of lncRNAs, miRNAs, and mRNAs in human TMJOA synovial tissues. By constructing lncRNA-related ceRNA networks using bioinformatics analysis, we aimed to probe their potential role in the development of TMJOA.

Materials and Methods

Sample details and collection

Patients with TMJOA were chosen as the experimental group. Since the synovium samples of healthy people cannot be collected due to ethical requirements, after patients were evaluated for clinical symptoms and imaging manifestations, we chose patients without any synovitis as controls. The inclusion criteria for the control group were as follows. (1) Patients with anterior disc displacement and in need of disc repositioning surgery; (2) Patients who had no clinical manifestations of pain; (3) Patients who had neither bony changes nor effusion. On the other hand, the inclusion criteria for the experimental group were as follows. (1) Patients with anterior disc displacement without reduction; (2) Patients who had clinical manifestations of pain; (3) Patients who had bony changes. Ten patients were enrolled for RNA seq (Table 1). Another 13 patients were enrolled for lncRNA expression verification (Table 2). During the collection operation, we cut the tissue in the posterior region of the articular disc, and carefully removed the surrounding muscle and fibrous layer. We then placed the sample in liquid nitrogen for preservation. The collection of all specimens was approved by the Ethics Committee of Shanghai Ninth People's Hospital (Shanghai, China). The protocol number is SH9H-2021-T141-1.

RNA sequencing

Total RNA was extracted from five TMJOA tissues and five control tissues using TRIzol reagent (Invitrogen, Carlsbad, CA, USA). All samples were tested for RNA concentration, purity, and integrity and qualified for RNA library construction. The RNA library was then sequenced by Cloud-seq Biotechnology (Shanghai, China).

Differential expression analysis and further screening of mRNAs

Differential expression (DE) analysis of lncRNAs, miRNAs, and mRNAs was performed by the DESeqDataSetFromMatrix function in the DESeq2 package (https://bioconductor.org/packages/release). DE RNAs with absolute log2FoldChange (FC) > 1 and p-value < 0.05 were selected using the dplyr: filter function in the tidyverse package (https://bioconductor.org/packages/release). Then all DE mRNAs were ranked and assigned according to log2FC, and the top 100 mRNAs were selected. TBtools (https://github.com/CJ-Chen/TBtools/releases) was used for differential gene heatmaps.

Pathway and functional analysis of differentially expressed mRNAs

Pathway and functional analysis of the top 100 ranked mRNAs was performed using the clusterProfiler package (https://bioconductor.org/packages/release). For the Kyoto

TABLE 1

Basic information of enrolled patients (whose samples were used for RNA sequencing)

Name	Hydrarthrosis	Articular disc & bone changes	Pain
OQY	Yes	Right-anterior disc displacement without reduction and with bony changes	Yes
ZXR	Yes	Bilateral-anterior disc displacement without reduction and with bony changes	Yes
SQ	Yes	Left-anterior disc displacement without reduction and with bony changes	Yes
LKK	Yes	Bilateral-anterior disc displacement without reduction and with bony changes	Yes
CWH	Yes	Right-anterior disc displacement without reduction and with bony changes	Yes
XXF	None	Bilateral-anterior disc displacement without reduction and without bony changes	None
FJY	None	Left-anterior disc displacement without reduction and without bony changes	None
SYL	None	Bilateral-anterior disc displacement without reduction and without bony changes	None
HYX	None	Left-anterior disc displacement without reduction and without bony changes	None
CLF	None	Right-anterior disc displacement without reduction and without bony changes	None

TABLE 2

Basic information of enrolled patients (samples used for lncRNA expression verification)

Name	Hydrarthrosis	Articular disc & bone changes	Pain
SFY	Yes	Bilateral-anterior disc displacement without reduction and with bony changes	Yes
WJM	Yes	Bilateral-anterior disc displacement without reduction and with bony changes	Yes
XRX	Yes	Bilateral-anterior disc displacement without reduction and with bony changes	Yes
QYN	Yes	Bilateral-anterior disc displacement without reduction and with bony changes	Yes
YLJ	Yes	Left-anterior disc displacement without reduction and with bony changes	Yes
RWY	Yes	Bilateral-anterior disc displacement without reduction and with bony changes	Yes
QXY	None	Left-anterior disc displacement without reduction and without bony changes	None
WSY	None	Right-anterior disc displacement without reduction and without bony changes	None
MM	None	Bilateral-anterior disc displacement without reduction and without bony changes	None
LRC	None	Bilateral-anterior disc displacement without reduction and without bony changes	None
WJY	None	Left-anterior disc displacement without reduction and without bony changes	None
QY	None	Right-anterior disc displacement without reduction and without bony changes	None
GBL	None	Bilateral-anterior disc displacement without reduction and without bony changes	None

Encyclopedia of Genes and Genomes (KEGG) analysis with the help of the enrichKEGG function and the enrichGO function for Gene Ontology (GO) analysis, pathways with p-value < 0.05 and gene ratio > 0.05 were selected. The bubble diagram and histogram were drawn with the Rgraphviz package (https://bioconductor.org/packages/release). For a more comprehensive analysis of all DE mRNAs, this study also utilized a gene set enrichment analysis (GSEA) to analyze all DE mRNAs with a p-value < 0.05 (without setting a threshold for fold change). After screening the pathways of interest, KEGG mapping tools (https://www.kegg.jp/) were used to draw the pathway diagram. The cytoHubba function in Cytoscape software (https://cytoscape.org/) was used to analyze the top 10 hub genes.

miRNA and lncRNA screening and ceRNA regulatory network construction

DE lncRNAs with fragments per kilobase of exon model per million mapped fragments (FPKM) values greater than 0 in the control and experimental groups were selected. Among them, intergenic lncRNAs (lincRNAs) with sequences that did not overlap with any known gene exons were used for further analysis. Upstream regulatory miRNAs capable of regulating the top 100 mRNAs were predicted using the FunRich software (http://www.funrich.org/), and the prediction results were intersected with DE miRNAs. The starBase database was used to predict upstream lncRNAs of selected miRNAs. Then, the intersection between predicted lncRNAs and the previously screened DE lincRNAs was determined. In this way, we constructed the complete lncRNA-miRNA-mRNA network in the range of DE significant RNAs (Fig. 1).

Preliminary validation of significant lncRNAs

SW982 cells were cultured in Leibovitz's L-15 medium supplemented with 10% fetal bovine serum (FBS). When the cell confluence reached 70%, TNF-a was added to the culture medium in a 5, 10, and 20 ng/ml concentration gradient. The cells were then cultured for another 48 h.

Interference of xist and grb2

Specific *xist* antisense oligonucleotide (ASO) and *grb2* small interfering RNA (si-RNA) was designed by Genomeditech (Shanghai, China) and transfected into SW982 cells using Lipofectamine 3000 transfection reagent (Thermo Fisher Scientific, Waltham, MA, USA). The primer sequences of *xist* were as follows:

Forward primer: ACCACACGTCAAGCTCTTCAT.
Reverse primer: CCTCAAGTGCTAGAGTGCCA.

RNA extraction and reverse transcription-quantitative polymerase chain reaction analysis

Total RNA was extracted from cells and tissues with Trizol reagent. Reverse transcription was performed using the Hifair® III 1st Strand cDNA Synthesis Kit (Yeasen, Shanghai, China). Then the reactions were subsequently measured on a Roche LightCycler®480II PCR instrument (Basel, Switzerland). All reactions were analyzed in triplicate. LncRNA expression was normalized to beta-actin (ACTB), and relative lncRNA expression levels were calculated using the $2^{-\Delta\Delta t}$ method.

Western blotting analysis

Cells were lysed in lysis buffer supplemented with protease inhibitors for 30 min on ice. Protein fractions were collected by centrifugation at 10,000×g for 10 min, separated on 10% sodium dodecyl-sulfate polyacrylamide gel electrophoresis (SDS-PAGE) gels, and then electrotransferred onto nitrocellulose membranes (Whatman, Piscataway, NJ, USA). Membranes were blocked with 5% bovine serum albumin (BSA) and then incubated with specific antibodies overnight at 4°C. The primary antibodies used were as follows: matrix

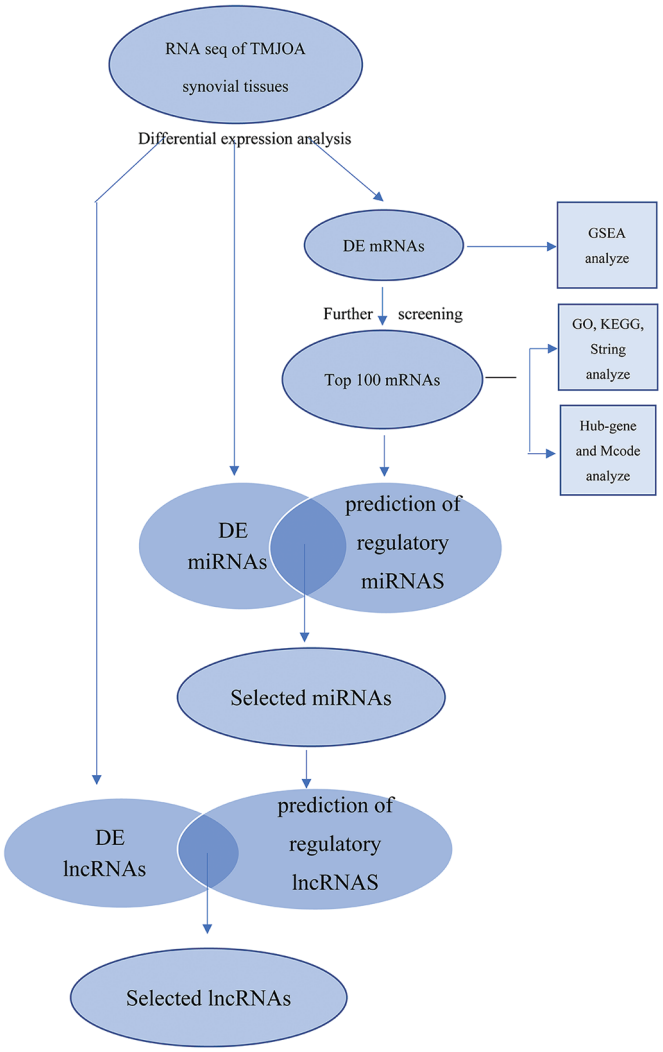

FIGURE 1. Schematic of this study.

metallopeptidase 13 (MMP13) (1:1000, 18165-1-AP, Proteintech), matrix metallopeptidase 3 (MMP3) (1:1000, abs130153, Absin), matrix metallopeptidase 2 (MMP2) (1:1000, ab86607, Abcam), AP-1 transcription factor subunit (c-FOS) (1:1000, A2444, Abclonal), cathepsin B (CTSB) (1:1000, A0967, Abclonal), growth factor receptor bound protein 2 (GRB2) (1:1000, A19059, Abclonal), and glyceraldehyde-3-phosphate dehydrogenase (GAPDH) (1:2000, AF7021, Affinity).

Cell proliferation assay

LncRNA was inhibited in SW982 cells under inflammatory stimuli, and fluorescence staining of proliferating cells was performed using the BeyoClick™EdU Cell Proliferation Kit with Alexa Fluor 488 (Beyotime Biotechnology, Shanghai, China) after 48 h of culture. Image acquisition was performed using a fluorescence microscope (Nikon, Japan).

Statistical analysis

All data from the control and experimental groups were analyzed using the paired two-tailed Student's *t*-test or two-way ANOVA. The statistical difference was set as $p < 0.05$.

Results

Basic patient information

A total of 10 female patients were enrolled, including 5 patients in the experimental group with a mean age of 35.0 ± 15.7 years and 5 patients in the control group with a mean age of 39.6 ± 15.8 years. A total of another 13 female patients were enrolled for lncRNA expression verification, including 6 patients (8 synovial tissues) in the experimental group with a mean age of 25.4 ± 17.0 years and 7 patients (8 synovial tissues) in the control group with a mean age of 23.1 ± 15.6 years. The basic information about the enrolled patients is provided in Tables 1 and 2.

Quality of RNA and the library

The A260/280 of RNA from all samples ranged from 1.8 to 2.0, indicating that the total RNA had high purity. The total amount of RNA extracted from each sample was ≥0.5 μg, which met the criteria and sequencing requirements. The bands of 28S and 18S rRNA in gel electrophoresis were clear, and the intensity of 28S rRNA was approximately twice that of 18S rRNA, suggesting that the extracted RNA had no genomic DNA (gDNA) contamination. The library

quality control results met the sequencing requirements. Our source data have been uploaded to GSE205389 and GSE205684.

Differential expression analysis and further screening of differentially expressed mRNAs

In this study, we found a total of 384 DE lncRNAs (upregulated 200, downregulated 184), 115 DE miRNAs (upregulated 33, downregulated 82), and 1767 DE mRNAs (upregulated 1158, downregulated 609). The volcano plot documented the differential expression of the three outcomes in TMJOA (Figs. 2A–2C). The heatmap showed the difference in expression of the top 100 upregulated/downregulated DE mRNAs between the two groups (Fig. 2D and Suppl. Fig. S1A).

Pathway and functional analysis of selected differentially expressed mRNAs

KEGG analysis showed that upregulated genes were mainly enriched in immune-related pathways. In addition, the osteoclast differentiation pathway was also enriched (Fig. 3A). Downregulated genes were mainly enriched in the cytoskeleton-regulated pathway (Suppl. Fig. S1B). The top 5 pathways ($p < 0.05$) enriched in GSEA were shown in Suppl. Fig. S1C. The GSEA analysis also showed osteoclast differentiation pathway similar to the KEGG analysis (Fig. 3B). The schematic of the osteoclast differentiation pathway has been illustrated with the relevant mRNAs involved in this pathway (Suppl. Fig. S1D).

By comparing GSEA with KEGG analysis results, it was shown that the main involved genes in each pathway were upregulated mRNAs, so we further analyzed the upregulated mRNAs and their upstream regulated miRNAs and lncRNAs. GO analysis showed that the upregulated genes mostly involved immune regulation-related biological processes such as antigen processing and presentation (Fig. 3C). Hub gene analysis further revealed the top 10 hub genes in upregulated mRNAs (Fig. 3D).

miRNA and lncRNA screening and ceRNA regulatory network construction

Among the 384 DE lncRNAs, 25 met the screening conditions (11 upregulated and 14 downregulated) (Table 3). A total of 15 downregulated DE miRNAs could constitute a regulatory relationship with DE mRNAs, of which 6 could simultaneously bind to DE lncRNAs (Fig. 4A). The results showed that among the upregulated DE lncRNAs, only one lncRNA, *xist*, could regulate 6 DE miRNAs: *miR-125b-5p*, *miR-1271-5p*, *miR-195-5p*, *miR-365a-3p*, *miR-27b-3p*, and *miR-199a-3p* (Fig. 4B). Further, these 6 downregulated miRNAs could form regulatory relationships with 9 upregulated mRNAs, including *ctsb*, *lcp1*, *mt2a*, *mmp3*, *fos*, *grb2*, *cd163*, *vamp8*, and *wdr1* (Fig. 4C).

Expression and functional verification of xist

RT-qPCRresults showed that the *xist* expression in TMJOA synovial tissue was about 3-fold higher than in the control group (Fig. 5A). Under 20 ng/ml TNF-a stimulation, the expression of *xist* in SW982 cells increased by about 2.6 times (Fig. 5B). Western blotting results showed that under the same concentration of TNF-a stimulation, the expression of CTSB, c-FOS and GRB2 protein in synovial cells increased, and cells secreted more MMP3, promoting matrix degradation (Fig. 5C). We screened the effective concentration of ASO-*xist*, and RT-qPCR results showed that the minimal effective dose was 100 nM. The *xist* expression was reduced by about 50% (Fig. 5D). Western blotting results showed that, under 20 ng/ml TNF-a stimulation, the protein expression levels of target genes in the network, including CTSB, c-FOS, and GRB2 were lowered with diminished *xist* levels. In the meantime, synovial cells produced less MMP3 and MMP13 (Fig. 5E). EdU fluorescence staining showed that *xist* also affected cell proliferation. Upon TNF-a stimulation, the cell proliferation rate reduced significantly in the ASO-NC group while the cell proliferation rate of the ASO-*xist* group only reduced slightly (Fig. 5F). Since GRB2 levels dropped most significantly when *xist* was inhibited, we further tested the function of GRB2. Western blotting showed that under 20 ng/ml TNF-a stimulation, the synthesis of a series of matrix degrading enzymes was blocked after GRB2 was inhibited (Fig. 5G).

Discussion

LncRNAs are noncoding RNAs of more than 200 nucleotides in length (Xie *et al.*, 2021). They can work as miRNA sponges to participate in regulating gene expression (Wang *et al.*, 2019c; Wu *et al.*, 2020). There is ample evidence that the relationship between lncRNAs and miRNAs plays an important role in OA progression (Xie *et al.*, 2020). For example, Zhang *et al.* (2019) found that lncRNA *malat1* could play a role in knee osteoarthritis by regulating chondrocyte proliferation, apoptosis, and extracellular matrix degradation through *miR-150-5p/akt3*. In another study, Liu *et al.* (2018) found that exosomes secreted by human stem cells contain lncRNA *klf3-as1*, which could regulate *miR-206/git1*, thereby affecting chondrocyte apoptosis. In addition, the lncRNA *malat1/miR-146a-PI3K/Akt/mTOR* axis and lncRNA *foxd2-as1/miR-27a-3p/tlr4* axis have also been reported to regulate chondrocyte matrix degradation (Wang *et al.*, 2019a; Li *et al.*, 2020b). Some scholars have sequenced lncRNAs and analyzed differentially expressed lncRNAs in knee OA cartilage tissues, providing a basis for studying the regulatory role of lncRNAs in knee OA cartilage degeneration (Fu et al., 2015; Liu *et al.*, 2016). As the initiating factor of OA, synovial inflammation can lead to the secretion of various inflammatory factors to promote cartilage degeneration, which is closely related to the severity and progression of OA (Kortekaas *et al.*, 2016; Bhattaram and Chandrasekharan, 2017; van den Bosch, 2019). Many scholars have therefore also conducted many aspects of research on OA synovial inflammation. For example, Xiang *et al.* (2019) identified differentially expressed circRNAs in synovial tissues of knee OA by RNA sequencing, while further validation is however needed. This study previously identified differentially expressed circRNAs in TMJOA synovial tissues and found that circRNA_*gcn1l1* was able to regulate TNF-a secretion in the synovium through *miRNA-*

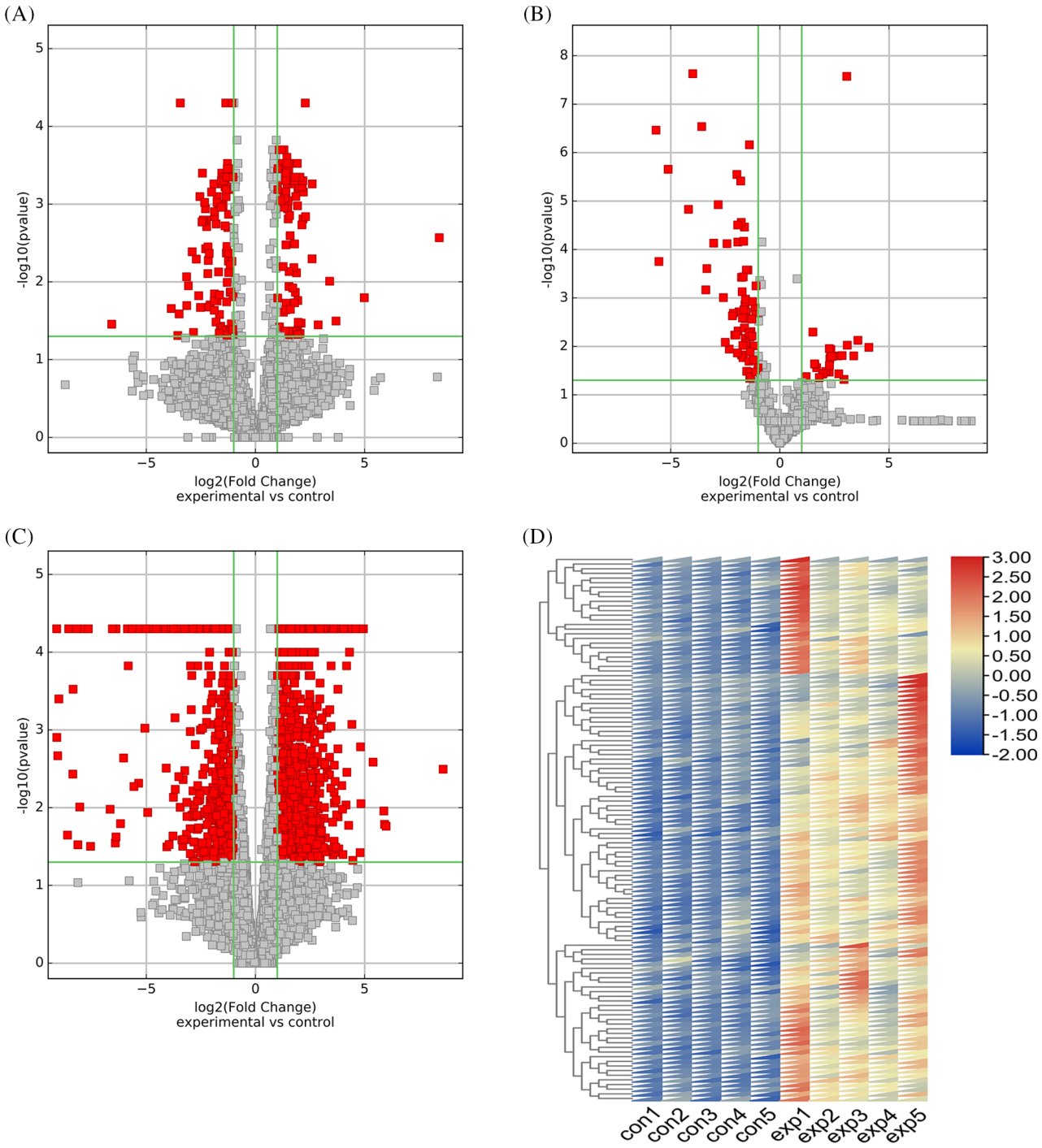

FIGURE 2. Differential expression of lncRNAs, miRNAs and mRNAs and further screening of differentially expressed (DE) mRNAs. Volcano plot of differentially expressed lncRNAs (A). Volcano plot of differentially expressed miRNAs (B). Volcano plot of differentially expressed mRNAs (C). Differential expression of top 100 upregulated mRNAs (D).

330-3p. Additionally, Xu *et al.* (2016) performed miRNA sequencing in TMJOA synovial tissues and found that *miR-221-3p* could regulate IL-1B and MMP1/9 secretion. However, none of the above studies involved the role of lncRNAs in OA and synovial inflammation symptoms. Studies on the relationship between lncRNAs and synovial inflammation have mostly come from RA. For example, Zou *et al.* (2018) sequenced lncRNAs in RA synovial tissue and found that lncRNA *lerfs* has a protective role in RA. Due to the current lack of reports of lncRNA regulation in TMJOA synovitis, we conducted lncRNA, miRNA, and mRNA sequencing in TMJOA synovial tissues in the hope of finding lncRNA/miRNA/mRNA axes that may play an important role in TMJOA.

The results of this study revealed that only one lncRNA molecule *xist*, was predicted to affect the expression of DE mRNAs through DE miRNAs.

LncRNA *xist* classically functions to silence the X chromosome to compensate for differences in the expression of X chromosome-associated genes between males and

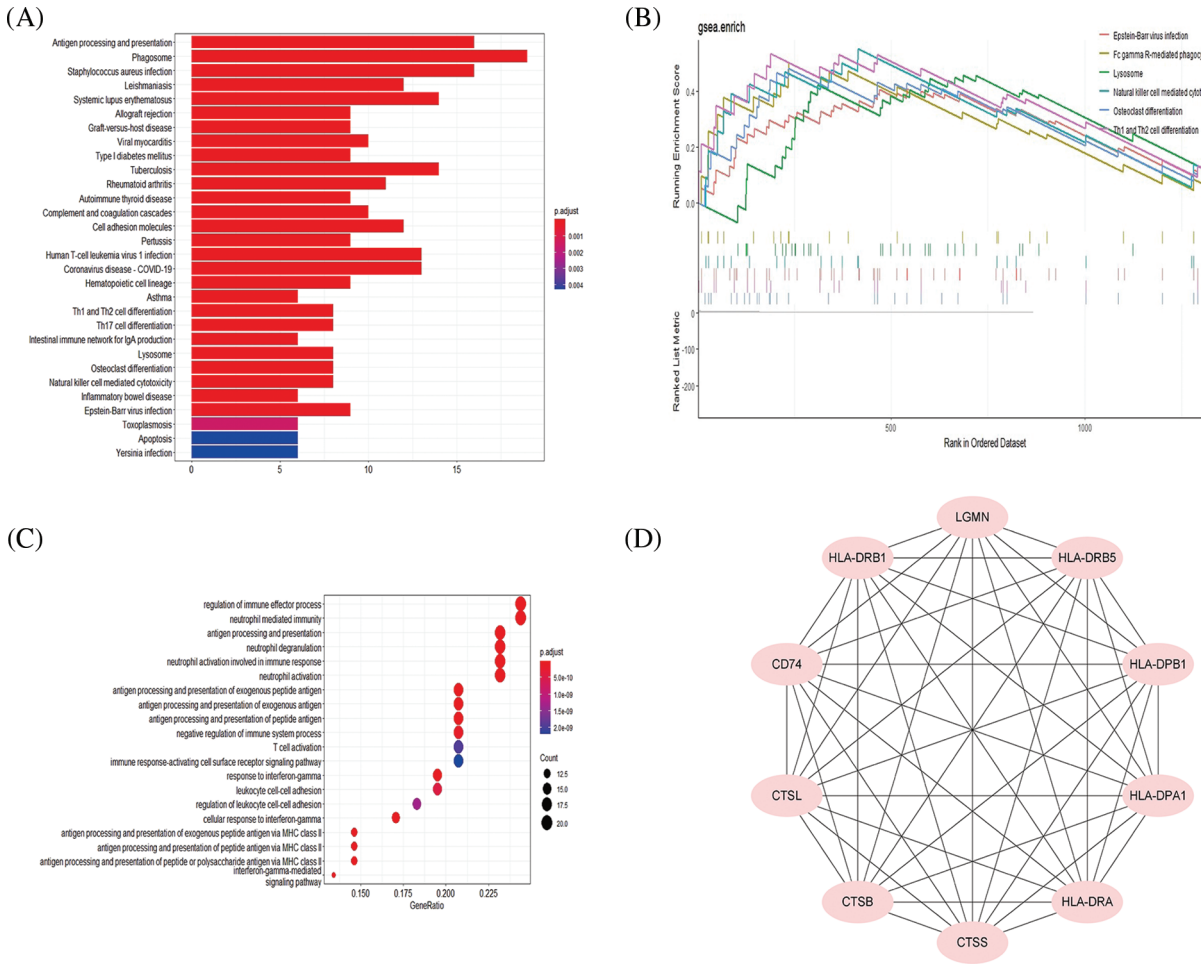

FIGURE 3. Pathway and functional analysis of top 100 upregulated mRNAs. Kyoto Encyclopedia of Genes and Genomes (KEGG) analysis of top 100 up-regulated mRNAs (A). The osteoclast differentiation pathway was also enriched in the gene set enrichment analysis (GSEA) analysis (B). Biological Process analysis of top 100 upregulated mRNAs (C). Hub genes of top 100 upregulated mRNAs (D).

TABLE 3

The basic information of differentially expressed (DE) lncRNAs which matched the criteria in our study

Name	Log2FC	*p*-value	Regulation
ENST00000602587	12.9726	0.0332	Up
ENST00000569008	4.07086	0.03405	Up
ENST00000605999	3.94441	0.0479	Up
ENST00000608741	3.83167	0.03785	Up
TCONS_00013978	3.78683	0.00635	Up
AK124533	3.75847	0.00535	Up
ENST00000596234	3.66798	0.00655	Up
ENST00000578929	3.44442	0.00765	Up
TCONS_00029691	3.17962	0.04455	Up
ENST00000365494	2.28194	0.00005	Up
TCONS_00029193	1.37479	0.00085	Up
ENST00000489090	−12.7334	0.0351	Down
ENST00000553177	−8.52903	0.04895	Down
AF088045	−4.51603	0.0041	Down
NR_026954	−3.29685	0.01015	Down

(Continued)

Table 3 (continued)

Name	Log2FC	*p*-value	Regulation
uc001zav.1	−3.08863	0.0499	Down
TCONS_00026354	−2.77091	0.0329	Down
ENST00000458468	−1.93027	0.0263	Down
ENST00000568248	−1.69983	0.01555	Down
ENST00000452320	−1.55396	0.0005	Down
ENST00000607056	−1.42903	0.0076	Down
ENST00000411553	−1.42595	0.04085	Down
ENST00000602813	−1.36281	0.00005	Down
uc004coz.1	−1.30393	0.00035	Down
ENST00000603037	−1.10313	0.04835	Down

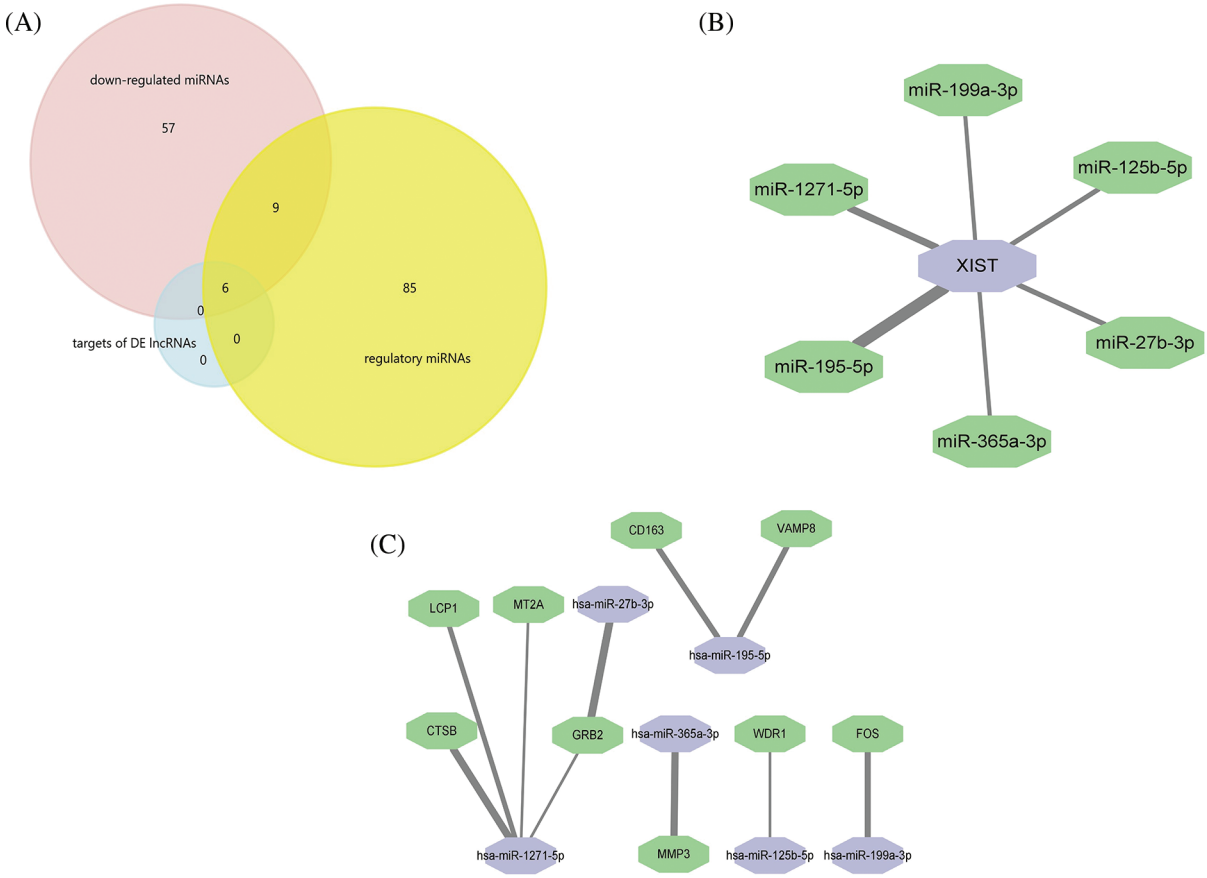

FIGURE 4. Professional website prediction showed upstream regulatory miRNAs and lncRNAs. Six down-regulated differentially expressed (DE) miRNAs were capable of forming regulatory relationships with DE mRNAs as well as DE lncRNAs (A). LncRNA *xist* could regulate six down-regulated DE miRNAs, the thicker the line, the greater the possibility of connection (B). LncRNA *xist* could regulate 9 DE mRNAs through 6 down-regulated DE miRNAs: the thicker the line, the greater the possibility of connection (C).

females (Czermiński and Lawrence, 2020). It can also play a role as an oncogene in some parenchymal tumors, including lung cancer and liver cancer (Yang *et al.*, 2020). CeRNA network-related research is also mainly in the field of oncology. For instance, Li *et al.* (2020a) found that *xist* was significantly increased in both synovial and cartilage tissues of knee OA, which was consistent with the results of the analysis in this paper. They found that *xist* could help express osteopontin (OPN) in M1 macrophages in synovial tissues by binding *miR-376c-5p*, promoting macrophage cytotoxicity to chondrocytes, and then resulting in chondrocyte apoptosis. In another report, Liu *et al.* (2020) also confirmed that there was a significant upregulation of *xist* in knee OA cartilage and found that *xist* could facilitate

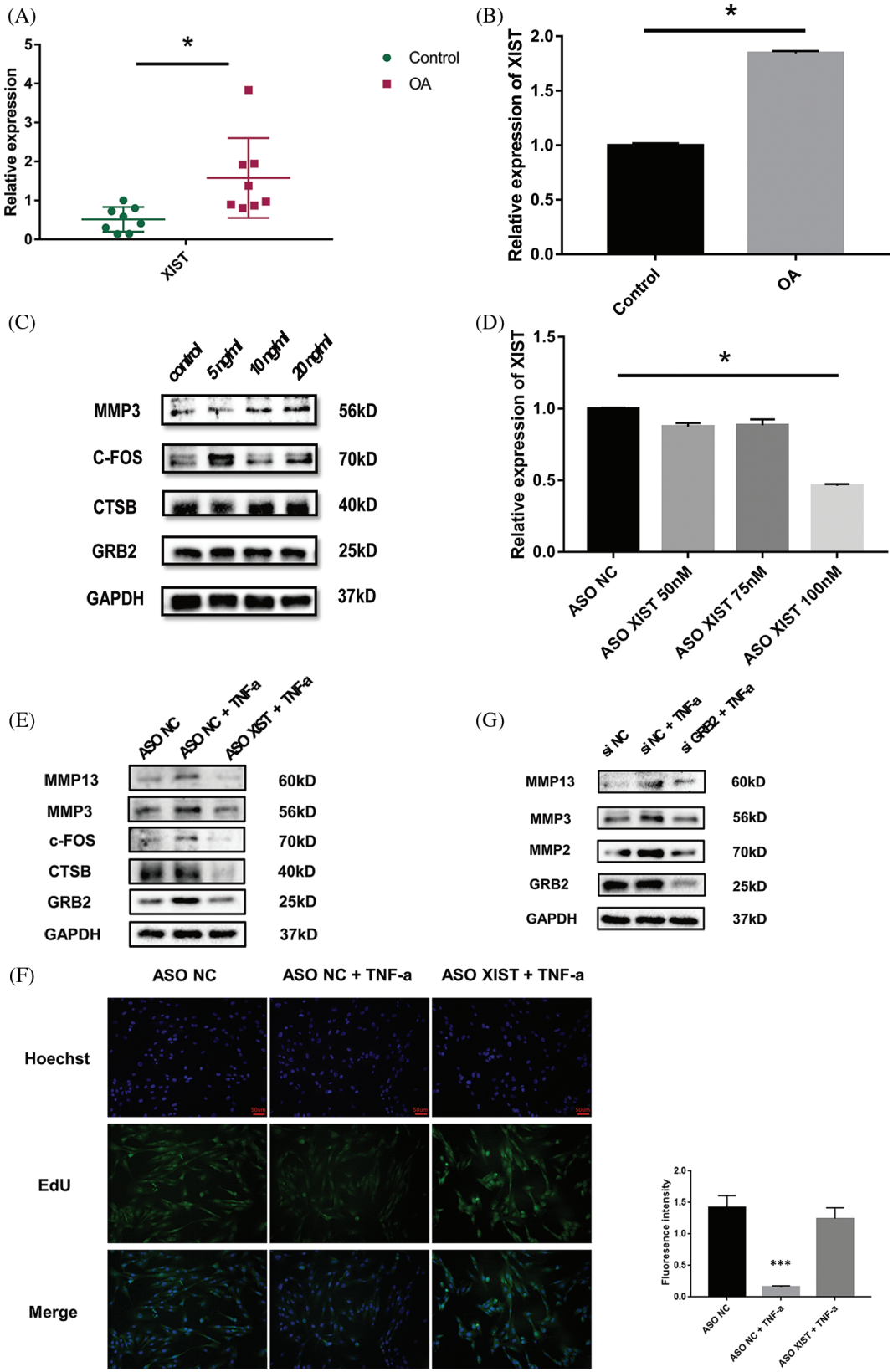

FIGURE 5. Expression profile and functional verification of *xist*. Reverse transcription-quantitative polymerase chain reaction (RT-qPCR) results showed that the *xist* expression in TMJOA synovial tissue was about 3-fold higher than in the control group (A). RT-qPCR results showed that upon TNF-a stimulation, the expression of *xist* in SW982 increased about 2.6 times (B). Western blot results showed that upon TNF-a stimulation, the expression of CTSB, c-FOS, and GRB2 protein in synovial cells increased, and cells secreted more MMP3 (C). RT-qPCR results showed that the minimal effective dose of ASO-*xist* was 100 nM, *xist* expression was reduced by about 50% (D). Western blot results showed that upon TNF-a stimulation, CTSB, c-FOS, and GRB2 decreased upon *xist* inhibition. In the meantime, synovial cells produced less MMP3 and MMP13 (E). EdU fluorescence staining showed that under TNF-a stimulation, the cell proliferation rate of the ASO-*xist* group was much higher than in the ASO-NC group (F). Western blotting showed that under TNF-a stimulation, the synthesis of a series of matrix degrading enzymes was blocked after GRB2 was inhibited (G). *, $p < 0.05$; ***, $p < 0.001$.

DNA methyltransferase 3A (DNMT3A) expression and eventually exacerbate the destruction of chondrocytes by inhibiting *miR-149-5p*. Further, Wang *et al.* (2019b) reported that significant upregulation of *xist* was also confirmed in knee OA cartilage, and the *xist/miR-1277-5p/mmp 13/adamts5* axis was found to have an important role in regulating OA disease development. Hence, *xist* can impact the course of OA through different targets and therefore may become an important target for the treatment of OA. Among lncRNAs, *xist* is a research hotspot with important functions. However, as most of the above studies were on cartilage tissue, the role of *xist* in synovitis is still unclear. Our *in vitro* experiments proved that blocking *xist* could protect synovial cells under inflammatory conditions.

Among the nine DE mRNAs predicted to be regulated by *xist*, *ctsb* was the hub gene selected by analysis, and *mmp3* is considered an important cartilage matrix degradation marker. Besides, *fos* and *grb2* products are molecules involved in the osteoclast differentiation pathway. The remaining five target genes are not involved in pathway enrichment or hub gene prediction. Thus *ctsb*, *mmp3*, *fos*, and *grb2* were screened as subsequent research points in this work. The known functions of these four mRNAs in TMJOA have been summarized in Table 4. Our primary results showed that under inflammatory conditions, protein expression of CTSB, MMP3, c-FOS, and GRB2 decreases after inhibition of *xist*. This provided the evidence for our network construction.

Cathepsin B (CTSB), a lysosomal cysteine protease, is also a marker of the dedifferentiated phenotype of chondrocytes (Li *et al.*, 2017). Research revealed that the DE miRNA *hsa-miR-1271-5p* could regulate CTSB. Zhang *et al.* (2021) documented that in chondrocytes, *miR-140-5p* could attenuate OA cartilage destruction by inhibiting CTSB/NLRP3. Ben-Aderet *et al.* (2015) found that CTSB was significantly higher in the synovial fluid in OA. However, the mechanism of CTSB in synovial tissue and synovitis is still unclear, and the analysis in this study yielded that the ceRNA network *xist/miR-1271-5p/ctsb* may function in synovitis.

Matrix metalloproteinase-3 (MMP3) is a classical molecule involved in cartilage destruction that is able to directly degrade the cartilage extracellular matrix and cause cartilage destruction by activating MMP9. MMP3 expression is directly related to the degree of inflammatory cell infiltration in the synovium. Further, increased metalloproteinase levels such as MMP3 are typical findings in OA (Berenbaum and Sellam, 2010). We found that the DE miRNA *miR-365a-3p*, a target of *xist*, was able to inhibit MMP3. It, therefore, constitutes the second ceRNA network, *xist/miR-365a-3p/mmp3*, in this study.

The results of GSEA and KEGG analysis both showed that the osteoclast differentiation pathway and osteoclast formation play an important role in the degeneration of subchondral bone (Zhu *et al.*, 2019). This may be a bridge between synovitis and pathological remodeling of the subchondral bone. There are two core genes, *fos* and *grb2* in the osteoclast differentiation pathway. The *fos*-encoded C-FOS protein is an important transcription factor in osteoclast formation, which is activated by the classical osteoclast formation regulator Receptor activator of nuclear factor kappa-B ligand (RANKL) and then activates the downstream NFATC1. Together with transcription factors such as MYC and NF-κB, C-FOS forms a complex network to function in promoting osteoclast formation. However, in this process, the regulation of C-FOS expression after activation by RANKL is not fully understood (Fujii *et al.*, 2021). Therefore, whether C-FOS is also regulated by other molecules and thus affects its final expression needs to be confirmed. We found that the DE miRNA *miR-199a-3p* is able to bind *fos*, so it is worth exploring whether *xist/miR-199a-3p* can play a role in osteoclast formation through *fos* and whether it can be a therapeutic target for TMJOA.

GRB2 is a key factor in several tyrosine kinase signaling conversion pathways. Some studies have reported that GRB2 can promote osteoclast survival by activating Erk and can strengthen the adhesion of osteoclasts to the bone surface, leading to bone resorption (Levy-Apter *et al.*, 2014). A recent study found that after the knockout of PIP5k1β kinase, GRB2 expression increased, and the ERK1/2 signaling pathway was more active, which promoted osteoclast formation (Zhao *et al.*, 2020). Our preliminary *in vitro* experiments demonstrated that under inflammatory conditions, inhibition of GRB2 contributes to the decline of

TABLE 4

The known functions of selected differentially expressed (DE) mRNAs in TMJOA

mRNA	Related reports in TMJOA
ctsb	There is still a lack of CTSB reports in TMJOA. A study has shown that in keen joint OA, CTSB could aggravate cartilage destruction (Zhang *et al.*, 2021).
mmp3	MMP3 is a classical molecule involved in cartilage destruction that is able to directly degrade cartilage extracellular matrix and cause cartilage destruction (Du *et al.*, 2021).
fos	There are a few reports about fos in TMJOA. However, in knee joint OA, studies have shown that, together with transcription factors such as MYC and NF-κB, C-FOS forms a complex network to function in promoting osteoclast formation (Fujii *et al.*, 2021).
grb2	There are few research papers on GRB2 in TMJOA. Some studies have reported that GRB2 can promote osteoclast survival by activating Erk and can strengthen the adhesion of osteoclasts to the bone surface, leading to bone resorption (Levy-Apter *et al.*, 2014).

matrix degrading enzymes in synoviocytes. This provides a research basis for alleviating joint destruction by regulating GRB2.

Through the bioinformatics analysis above, four ceRNA regulatory axes were found in this study, including *xist/miR-1271-5p/ctsb*, *xist/miR-365a-3p/mmp3*, *xist/miR-199a-3p/fos*, and *xist/miR-27b-3p/miR-1271-5p/grb2*. These four networks may be involved in the development of synovial inflammation and are one of the important reasons why synovial inflammation can promote cartilage and subchondral bone degeneration. Their roles still need to be confirmed by further *in vitro* and *in vivo* studies. Thus, in our future work, we will focus on the validation of the aforementioned ceRNA networks.

Funding Statement: This study was supported by grants from the National Natural Science Foundation of China (32071313, 82270996), the Science and Technology Commission of Shanghai Municipality Science Research Project (20S31902500, 20Y11903900), and the Cross-Disciplinary Research Fund of Shanghai Ninth People's Hospital, Shanghai Jiao Tong University School of Medicine (JYJC202203).

Author Contributions: The authors confirm contribution to the paper as follows: study conception and design: Dongmei He; data collection: Chuyao Wang; analysis and interpretation of results: Chuyao Wang, Chuan Lu; draft manuscript preparation: Luxiang Zou. All authors reviewed the results and approved the final version of the manuscript.

Availability of Data and Materials: All data generated or analyzed during this study are included in this published article (and its supplementary information files).

Ethics Approval: The collection of all specimens was approved by the Ethics Committee of Shanghai Ninth People's Hospital (Shanghai, China). The protocol number is SH9H-2021-T141-1 and the date of adoption was June 01, 2021. All patients signed an informed consent approved by the Institutional Review Board.

Conflicts of Interest: The authors declare that they have no conflicts of interest to report regarding the present study.

References

Ben-Aderet L, Merquiol E, Fahham D, Kumar A, Reich E et al. (2015). Detecting cathepsin activity in human osteoarthritis via activity-based probes. *Arthritis Research & Therapy* **17**: 1–14. https://doi.org/10.1186/s13075-015-0586-5

Berenbaum F, Sellam J (2010). The role of synovitis in pathophysiology and clinical symptoms of osteoarthritis. *Nature Reviews Rheumatology* **6**: 625–635. https://doi.org/10.1038/nrrheum.2010.159

Bhattaram P, Chandrasekharan U (2017). The joint synovium: A critical determinant of articular cartilage fate in inflammatory joint diseases. *Seminars in Cell & Developmental Biology* **62**: 86–89. https://doi.org/10.1016/j.semcdb.2016.05.009

Bi X, Guo XH, Mo BY, Wang ML, Luo XQ, Chen YX, Liu F, Olsen N, Pan YF, Zheng SG (2019). LncRNA PICSAR promotes cell proliferation, migration and invasion of fibroblast-like synoviocytes by sponging miRNA-4701-5p in rheumatoid arthritis. *eBioMedicine* **50**: 408–420. https://doi.org/10.1016/j.ebiom.2019.11.024

Bush JR, Beier F (2013). TGF-β and osteoarthritis–The good and the bad. *Nature Medicine* **19**: 667–669. https://doi.org/10.1038/nm.3228

Czerminski JT, Lawrence JB (2020). Silencing trisomy 21 with XIST in neural stem cells promotes neuronal differentiation. *Developmental Cell* **52**: 294–308. https://doi.org/10.1016/j.devcel.2019.12.015

Du S, Liang C, Sun Y, Ma B, Gao W, Geng W (2021). The attenuating effect of low-intensity pulsed ultrasound on hypoxia-induced rat chondrocyte damage in TMJ osteoarthritis based on TMT labeling quantitative proteomic analysis. *Frontiers in Pharmacology* **12**: 752734. https://doi.org/10.3389/fphar.2021.752734

Fu M, Huang G, Zhang Z, Liu J, Zhang Z, Huang Z, Yu B, Meng F (2015). Expression profile of long noncoding RNAs in cartilage from knee osteoarthritis patients. *Osteoarthritis and Cartilage* **23**: 423–432. https://doi.org/10.1016/j.joca.2014.12.001

Fu X, Song G, Ni R, Liu H, Xu Z, Zhang D, He F, Huang G (2021). LncRNA-H19 silencing suppresses synoviocytes proliferation and attenuates collagen-induced arthritis progression by modulating miR-124a. *Rheumatology* **60**: 430–440. https://doi.org/10.1093/rheumatology/keaa395

Fujii T, Murata K, Mun S, Bae S, Lee YJ, Pannellini T, Kang K, Oliver D, Park-Min KH, Ivashkiv LB (2021). MEF2C regulates osteoclastogenesis and pathologic bone resorption via c-FOS. *Bone Research* **9**: 4. https://doi.org/10.1038/s41413-020-00120-2

Kortekaas MC, Kwok W, Reijnierse M, Stijnen T, Kloppenburg M (2016). Brief report: Association of inflammation with development of erosions in patients with hand osteoarthritis: A prospective ultrasonography study. *Arthritis & Rheumatology* **68**: 392–397. https://doi.org/10.1002/art.39438

Kostopoulou F, Malizos KN, Papathanasiou I, Tsezou A (2015). MicroRNA-33a regulates cholesterol synthesis and cholesterol efflux-related genes in osteoarthritic chondrocytes. *Arthritis Research & Therapy* **17**: 1–13. https://doi.org/10.1186/s13075-015-0556-y

Levy-Apter E, Finkelshtein E, Vemulapalli V, Li SSC, Bedford MT, Elson A (2014). Adaptor protein GRB2 promotes src tyrosine kinase activation and podosomal organization by protein-tyrosine phosphatase ε in osteoclasts. *Journal of Biological Chemistry* **289**: 36048–36058. https://doi.org/10.1074/jbc.M114.603548

Li Y, Fang J, Ao G (2017). Cathepsin B and L inhibitors: A patent review (2010-present). *Expert Opinion on Therapeutic Patents* **27**: 643–656. https://doi.org/10.1080/13543776.2017.1272572

Li H, Guo H, Lei C, Liu L, Xu LQ et al. (2019). Nanotherapy in joints: Increasing endogenous hyaluronan production by delivering

hyaluronan synthase 2. *Advanced Materials* **31**: 1904535. https://doi.org/10.1002/adma.201904535

Li L, Lv G, Wang B, Kuang L (2020a). XIST/miR-376c-5p/OPN axis modulates the influence of proinflammatory M1 macrophages on osteoarthritis chondrocyte apoptosis. *Journal of Cellular Physiology* **235**: 281–293. https://doi.org/10.1002/jcp.28968

Li H, Xie S, Li H, Zhang R, Zhang H (2020b). LncRNA MALAT1 mediates proliferation of LPS treated-articular chondrocytes by targeting the miR-146a-PI3K/Akt/mTOR axis. *Life Sciences* **254**: 116801. https://doi.org/10.1016/j.lfs.2019.116801

Liu Q, Hu X, Zhang X, Dai L, Duan X, Zhou C, Ao Y (2016). The TMSB4 pseudogene LncRNA functions as a competing endogenous RNA to promote cartilage degradation in human osteoarthritis. *Molecular Therapy* **24**: 1726–1733. https://doi.org/10.1038/mt.2016.151

Liu Y, Lin L, Zou R, Wen CY, Wang Z, Lin F (2018). MSC-derived exosomes promote proliferation and inhibit apoptosis of chondrocytes via lncRNA-KLF3-AS1/miR-206/GIT1 axis in osteoarthritis. *Cell Cycle* **17**: 2411–2422. https://doi.org/10.1080/15384101.2018.1526603

Liu Y, Liu K, Tang C, Shi Z, Jing K, Zheng J (2020). Long non-coding RNA XIST contributes to osteoarthritis progression via miR-149-5p/DNMT3A axis. *Biomedicine & Pharmacotherapy* **128**: 110349. https://doi.org/10.1016/j.biopha.2020.110349

Memczak S, Jens M, Elefsinioti A, Torti F, Krueger J, Rybak A, Rajewsky N (2013). Circular RNAs are a large class of animal RNAs with regulatory potency. *Nature* **495**: 333–338. https://doi.org/10.1038/nature11928

van den Bosch MHJ (2019). Inflammation in osteoarthritis: Is it time to dampen the alarm(in) in this debilitating disease? *Clinical and Experimental Immunology* **195**: 153–166. https://doi.org/10.1111/cei.13237

Wang Y, Cao L, Wang Q, Huang J, Xu S (2019a). LncRNA FOXD2-AS1 induces chondrocyte proliferation through sponging miR-27a-3p in osteoarthritis. *Artificial Cells Nanomedicine Biotechnology* **47**: 1241–1247. https://doi.org/10.1080/21691401.2019.1596940

Wang P, Chen D, Ma H, Li Y (2017). LncRNA MEG3 enhances cisplatin sensitivity in non-small cell lung cancer by regulating miR-21-5p/SOX7 axis. *OncoTargets and Therapy* **10**: 5137–5149. https://doi.org/10.2147/OTT

Wang T, Liu Y, Wang Y, Huang X, Zhao W, Zhao Z (2019b). Long non-coding RNA XIST promotes extracellular matrix degradation by functioning as a competing endogenous RNA of miR-1277-5p in osteoarthritis. *International Journal of Molecular Medicine* **44**: 630–642. https://doi.org/10.3892/ijmm.2019.4240

Wang K, Long B, Liu F, Wang J, Liu CY, Zhao B, Zhou LY, Sun T, Wang M, Yu T (2016). A circular RNA protects the heart from pathological hypertrophy and heart failure by targeting miR-223. *European Heart Journal* **37**: 2602–2611. https://doi.org/10.1093/eurheartj/ehv713

Wang M, Mao C, Ouyang L, Liu Y, Lai W et al. (2019c). Long noncoding RNA LINC00336 inhibits ferroptosis in lung cancer by functioning as a competing endogenous RNA. *Cell Death & Differentiation* **26**: 2329–2343. https://doi.org/10.1038/s41418-019-0304-y

Wang J, Zhao Q (2020). LncRNA LINC-PINT increases SOCS1 expression by sponging miR-155-5p to inhibit the activation of ERK signaling pathway in rheumatoid arthritis synovial fibroblasts induced by TNF-α. *International Immunopharmacology* **84**: 106497. https://doi.org/10.1016/j.intimp.2020.106497

Wu P, Mo Y, Peng M, Tang T, Zhong Y, Deng X, Xiong W (2020). Emerging role of tumor-related functional peptides encoded by lncRNA and circRNA. *Molecular Cancer* **19**: 1–14. https://doi.org/10.1186/s12943-020-1147-3

Xiang S, Li Z, Bian Y, Wei X (2019). RNA sequencing reveals the circular RNA expression profiles of osteoarthritic synovium. *Journal of Cellular Biochemistry* **120**: 18031–18040. https://doi.org/10.1002/jcb.29106

Xiao J, Wang R, Zhou W, Cai X, Ye Z (2021). LncRNA NEAT1 regulates the proliferation and production of the inflammatory cytokines in rheumatoid arthritis fibroblast-like synoviocytes by targeting miR-204-5p. *Human Cell* **34**: 372–382. https://doi.org/10.1007/s13577-020-00461-4

Xie J, Li H, Chen L, Cao Y, Hu Y, Zhu Z, Wang M, Shi J (2021). A novel pyroptosis-related lncRNA signature for predicting the prognosis of skin cutaneous melanoma. *International Journal of General Medicine* **14**: 6517–6527. https://doi.org/10.2147/IJGM.S335396

Xie F, Liu YL, Chen XY, Li Q, Zhong J, Dai BY, Shao XF, Wu GB (2020). Role of MicroRNA, LncRNA, and exosomes in the progression of osteoarthritis: A review of recent literature. *Orthopaedic Surgery* **12**: 708–716. https://doi.org/10.1111/os.12690

Xiong D, Li Z, Liang L, He R, Ma F, Luo D, Hu X, Chen G (2018). The LncRNA NEAT1 accelerates lung adenocarcinoma deterioration and binds to Mir-193a-3p as a competitive endogenous RNA. *Cellular Physiology and Biochemistry* **48**: 905–918. https://doi.org/10.1159/000491958

Xu J, Liu Y, Deng M, Li J, Cai H, Meng Q, Fang W, Long X, Ke J (2016). MicroRNA221-3p modulates Ets-1 expression in synovial fibroblasts from patients with osteoarthritis of temporomandibular joint. *Osteoarthritis and Cartilage* **24**: 2003–2011. https://doi.org/10.1016/j.joca.2016.06.011

Yang X, Zhang S, He C, Xue P, Zhang L, He Z, Zang L, Feng B, Sun J, Zheng M (2020). METTL14 suppresses proliferation and metastasis of colorectal cancer by down-regulating oncogenic long non-coding RNA XIST. *Molecular Cancer* **19**: 1–16. https://doi.org/10.1186/s12943-020-1146-4

Yin C, Suen W, Lin S, Wu XM, Li G, Pan XH (2017). Dysregulation of both miR-140-3p and miR-140-5p in synovial fluid correlate with osteoarthritis severity. *Bone Joint Research* **6**: 612–618. https://doi.org/10.1302/2046-3758.611.BJR-2017-0090.R1

Zhang L, Qiu J, Shi J, Liu S, Zou H (2021). MicroRNA-140-5p represses chondrocyte pyroptosis and relieves cartilage injury in osteoarthritis by inhibiting cathepsin B/Nod-like receptor protein 3. *Bioengineered* **12**: 9933–9948. https://doi.org/10.1080/21655979.2021.1985342

Zhang Y, Wang F, Chen G, He R, Yang L (2019). LncRNA MALAT1 promotes osteoarthritis by modulating miR-150-5p/AKT3 axis. *Cell & Bioscience* **9**: 1–12. https://doi.org/10.1186/s13578-019-0302-2

Zhao X, Cui P, Hu G, Wang C, Jiang L, Zhao J, Xu J, Zhang X (2020). PIP5k1β controls bone homeostasis through modulating both osteoclast and osteoblast differentiation. *Journal of Molecular Cell Biology* **12**: 55–70. https://doi.org/10.1093/jmcb/mjz028

Zheng Q, Bao C, Guo W, Li S, Chen J et al. (2016). Circular RNA profiling reveals an abundant circHIPK3 that regulates cell growth by sponging multiple miRNAs. *Nature Communications* **7**: 1–13. https://doi.org/10.1038/ncomms11215

Zheng L, Pi C, Zhang J, Fan Y, Cui C et al. (2018). Aberrant activation of latent transforming growth factor-beta initiates the onset of temporomandibular joint osteoarthritis. *Bone Research* **6**: 1–10. https://doi.org/10.1038/s41413-018-0027-6

Zhu H, Hu Y, Wang C, Zhang X, He D (2020). CircGCN1L1 promotes synoviocyte proliferation and chondrocyte apoptosis by targeting miR-330-3p and TNF-α in TMJ osteoarthritis. *Cell Death & Disease* **11**: 1–16. https://doi.org/10.1038/s41419-020-2447-7

Zhu S, Zhu J, Zhen G, Hu Y, An S et al. (2019). Subchondral bone osteoclasts induce sensory innervation and osteoarthritis pain. *Journal of Clinical Investigation* **129**: 1076–1093. https://doi.org/10.1172/JCI121561

Zou Y, Xu S, Xiao Y, Qiu Q, Shi M et al. (2018). Long noncoding RNA LERFS negatively regulates rheumatoid synovial aggression and proliferation. *Journal of Clinical Investigation* **128**: 4510–4524. https://doi.org/10.1172/JCI97965

Supplementary Materials

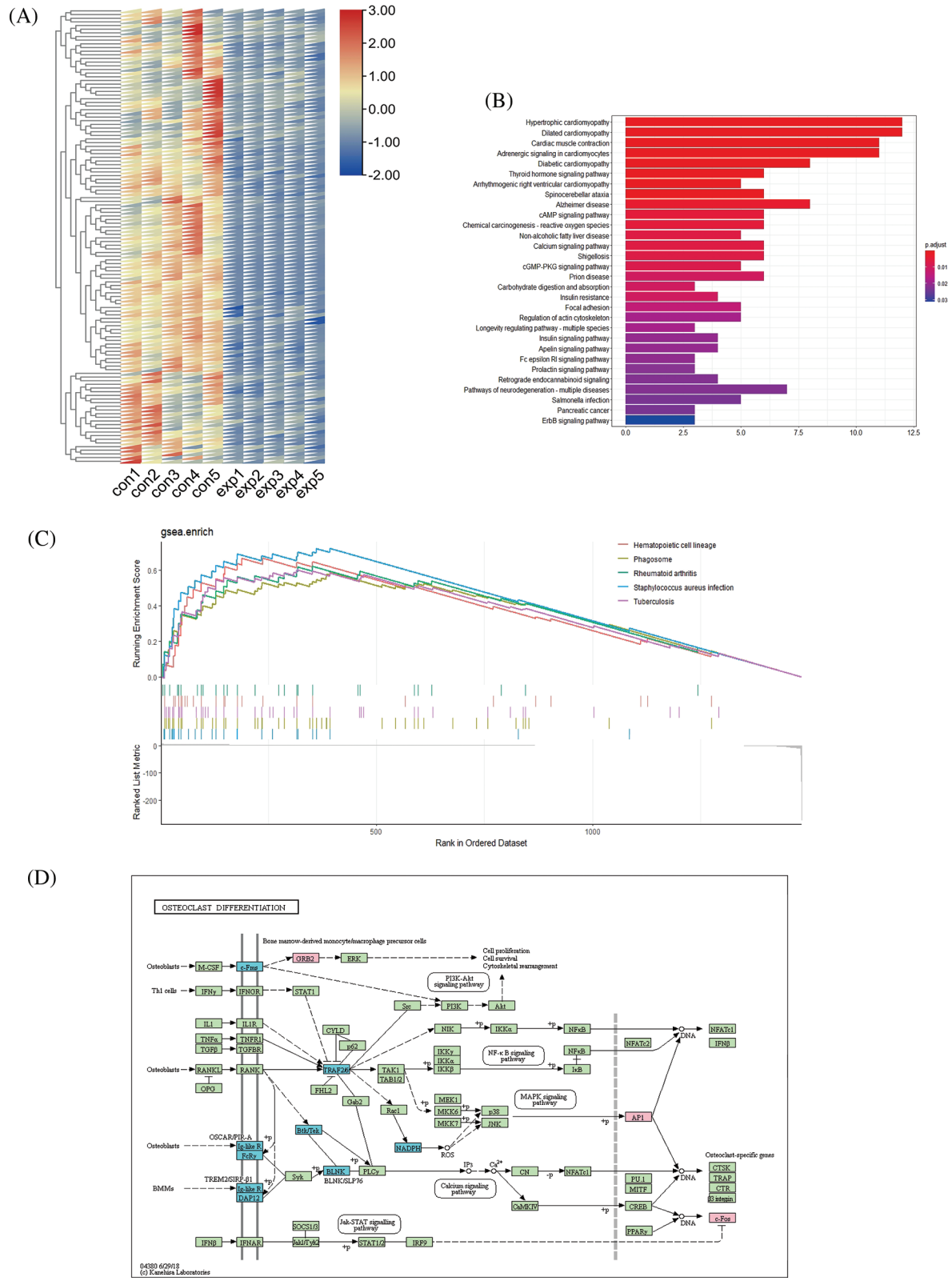

FIGURE S1. Details of pathway and functional analysis results of top 100 differentially expressed (DE) mRNAs. Differential expression of top 100 downregulated mRNAs between the experimental group and control group (A). Kyoto Encyclopedia of Genes and Genomes (KEGG) analysis of top 100 downregulated mRNAs (B). Top five pathways in the gene set enrichment analysis (GSEA) analysis of all DE mRNAs with p value < 0.05 (C). Schematic diagram of the osteoclast differentiation pathway (D).